β-Amyloid peptides enhance α-synuclein accumulation and neuronal deficits in a transgenic mouse model linking Alzheimer's disease and Parkinson's disease

Eliezer Masliah*†‡, Edward Rockenstein*, Isaac Veinbergs†, Yutaka Sagara*, Margaret Mallory*, Makoto Hashimoto*, and Lennart Mucke§

Departments of *Neurosciences and †Pathology, University of California at San Diego, La Jolla, CA 92093; and §Gladstone Institute of Neurological Disease and Department of Neurology, University of California, San Francisco, CA 94141

Communicated by Robert W. Mahley, The J. David Gladstone Institutes, San Francisco, CA, August 6, 2001 (received for review May 8, 2001)

Alzheimer's disease and Parkinson's disease are associated with the cerebral accumulation of β-amyloid and α-synuclein, respectively. Some patients have clinical and pathological features of both diseases, raising the possibility of overlapping pathogenetic pathways. We generated transgenic (tg) mice with neuronal expression of human β-amyloid peptides, α-synuclein, or both. The functional and morphological alterations in doubly tg mice resembled the Lewy-body variant of Alzheimer's disease. These mice had severe deficits in learning and memory, developed motor deficits before α-synuclein singly tg mice, and showed prominent age-dependent degeneration of cholinergic neurons and presynaptic terminals. They also had more α-synuclein-immunoreactive neuronal inclusions than α-synuclein singly tg mice. Ultrastructurally, some of these inclusions were fibrillar in doubly tg mice, whereas all inclusions were amorphous in α-synuclein singly tg mice. β-Amyloid peptides promoted aggregation of α-synuclein in a cell-free system and intraneuronal accumulation of α-synuclein in cell culture. β-Amyloid peptides may contribute to the development of Lewy-body diseases by promoting the aggregation of α-synuclein and exacerbating α-synuclein-dependent neuronal pathologies. Therefore, treatments that block the production or accumulation of β-amyloid peptides could benefit a broader spectrum of disorders than previously anticipated.

Aging is a major risk factor for neurodegenerative disorders, such as Alzheimer's disease (AD) and Parkinson's disease (PD), and the number of people with these conditions is increasing rapidly. In the United States alone, an estimated 4 million people have AD and at least one million have PD. Within the next 40–50 years, these numbers are projected to increase to over 8 million for AD and to 4 million for PD. Each neurodegenerative disease appears to have a predilection for specific brain regions and cell populations. However, human cases with clinical and neuropathological features of both AD and PD (1–3) raise the possibility that these diseases involve overlapping pathways.

Many AD patients develop signs of PD and some PD patients become demented (3). Both diseases are associated with degeneration of neurons and interneuronal synaptic connections, depletion of specific neurotransmitters, and abnormal accumulation of misfolded proteins, whose precursors participate in normal central nervous system functions (4–11). The β-amyloid protein precursor (APP) and α-synuclein (SYN) are expressed abundantly in synapses, are well conserved across species, and have been implicated in neural plasticity, learning, and memory (6, 7, 12). Mutations in human APP (hAPP) that increase production of hAPP-derived β-amyloid peptides (Aβ) cause autosomal dominant forms of familial AD (FAD) (11), and expression of FAD-mutant hAPPs in neurons of transgenic (tg) mice results in the age-dependent development of AD-like central nervous system alterations (13–17). Mutations in human SYN (hSYN) that enhance hSYN aggregation have been identified in autosomal dominant forms of PD (18, 19). Although most patients with AD and PD have no mutations in hAPP or hSYN, even the most frequent "sporadic" forms of these diseases are associated with an abnormal accumulation of Aβ (10, 11) and hSYN (20–22), respectively. Aβ accumulates in extracellular amyloid plaques and probably also inside neurons, and hSYN accumulates in intraneuronal inclusions called Lewy bodies transgenic mice expressing wild-type hSYN in neurons develop neuronal accumulations of hSYN, loss of dopaminergic terminals in the basal ganglia, and motor impairments (23), all of which are hallmarks of PD. Neuronal expression of hSYN in fruit flies resulted in similar alterations (24). That neuronal accumulation of hSYN is associated with similar morphological and functional alterations in species as diverse as flies, mice, and humans is provocative and suggests that it may contribute to the development of PD and other Lewy-body diseases.

We hypothesized that hSYN and Aβ have distinct, as well as convergent, pathogenic effects on the integrity and function of the brain. hSYN might affect motor function more than cognitive function, whereas the opposite might be true for Aβ. In addition, hSYN and Aβ could interact more directly by engaging synergistic neurodegenerative pathways. To test these hypotheses, we generated tg mice that express hSYN either alone or in combination with hAPP/Aβ.

Methods

Generation and Behavioral Testing of Tg Mice. Heterozygous hSYN mice from line D (23) were crossed with heterozygous hAPP mice from line J9 (17). The offspring were genotyped (17, 23) and analyzed at 4–22 months of age. Before behavioral experiments, mice were singly housed to reduce effects of social stress. Mice had free access to food and water. Experiments were carried out during the light cycle. Locomotor activity was analyzed as described (23). Spatial learning and memory were assessed in a water maze test. A pool (diameter, 180 cm) was filled with opaque water (24°C), and mice were first trained to locate a visible platform (days 1–6) and then a submerged hidden platform (days 7–12) in three daily trials 2–3 min apart. Mice that failed to find the hidden platform within 90 s were put on it for 30 s. The same platform location was used for all sessions and all

Abbreviations: AD, Alzheimer's disease; PD, Parkinson's disease; APP, β-amyloid protein precursor; SYN, α-synuclein; hAPP, human APP; Aβ, β-amyloid peptides; FAD, familial AD; hSYN, human SYN; ChAT, choline acetyltransferase; SIPT, synaptophysin-immunoreactive presynaptic terminals of defined signal intensity; tg, transgenic.

‡To whom reprint requests should be addressed. E-mail: emasliah@ucsd.edu.

The publication costs of this article were defrayed in part by page charge payment. This article must therefore be hereby marked "*advertisement*" in accordance with 18 U.S.C. §1734 solely to indicate this fact.

mice. The starting point at which each mouse was placed into the water was changed randomly between two alternative entry points located at a similar distance from the platform. Time to reach the platform (latency), path length, and swim speed were recorded with a Noldus Instruments EthoVision video tracking system (San Diego Instruments, San Diego) set to analyze two samples per second. On day 13, the platform was removed for a 30-s probe trial, during which we recorded the percent time the mouse spent in the quadrant of the pool that previously contained the platform (target quadrant) and in each of the nontarget quadrants. To control for differences in motivation or fatigue, the probe trial was followed by a trial with a visible platform. There were no significant differences in average swim speeds or path lengths between the different groups of mice during the latter trial (data not shown).

Quantitation of Transgene Products. hSYN and hAPP mRNA and protein levels were determined by RNase protection assay and Western blot analysis as described (23, 25), except the actin riboprobe was complementary to nucleotides 490–565 of mouse β-actin cDNA (GenBank accession no. X03672), and an actin antibody (MAB1501, Chemicon) was used to confirm equal loading of protein in the Western blot analysis.

For the determination of Aβ levels by ELISA, samples of mouse cortex were homogenized in ice-cold PBS containing 5 M guanidine·HCl and 1× protease inhibitor mixture (pH 8.0) (Calbiochem). Homogenates were mixed for 3–4 h at room temperature and centrifuged at 16,000 × g for 20 min at 4°C. The supernatant was diluted 10-fold in Dulbecco's PBS (pH 7.4) containing 5% BSA and 0.03% Tween 20. Aβ1–40 and Aβ1–42 levels in the diluted brain homogenates were quantitated with a sandwich ELISA (BioSource International, Camarillo, CA) according to the manufacturer's instructions.

Neuronal Cell Culture. Cells of the immortalized hypothalamic neuronal cell line GT1–7 (a gift from P. Mellon, University of California at San Diego) express neuronal markers, form synapses, produce neurotransmitters (26) and, on transfection with SYN, show mitochondrial alterations, inclusion body formation, evidence of oxidative stress, and synaptic dysfunction (27). Cells were stably transfected with SYN cDNA or control plasmid as described (27), plated in 24-well plates coated with poly-L-lysine (5×10^4/0.5 ml of DMEM with 10% serum and without G418), and treated with synthetic peptides from Sigma as outlined in Fig. 6. For quantitation of SYN-immunoreactive inclusions, coverslips were immunostained (27) and analyzed by light microscopy and computer-aided image analysis with a Quantimet 570C (Leica, Deerfield, IL). For each condition, five coverslips and an average of 20 cells per coverslip were analyzed. Results were expressed as percentage of cells with SYN-immunoreactive inclusions.

Neuropathological Analysis. Mice were euthanized by transcardial saline perfusion under anesthesia with chloral hydrate. Brains were removed and divided sagittally. The right hemibrain was snap-frozen and stored at −70°C for RNA or protein analysis. The left hemibrain was drop-fixed in phosphate-buffered 4% paraformaldehyde at 4°C for 48 h and serially sectioned sagittally at 40 μm with a Vibratome 2000 (Leica).

Immunohistochemical analysis was performed on free-floating Vibratome sections (17, 23) with anti-hSYN (72–10, 1:200) (23), anti-hAPP (clone 8E5, 1:1000, Elan Pharmaceuticals, San Francisco) (13), anti-Aβ (3D6, 1:600, Elan Pharmaceuticals) (28), anti-choline acetyltransferase (ChAT; AB143, 1:1000, Chemicon), and anti-synaptophysin (SY38, 1:10, Chemicon). The specificity of immunostaining results was confirmed by incubating sections or cells overnight with preimmune serum or without primary antibody. For double-labeling, sections were incubated overnight at 4°C with anti-hSYN (1:1000), followed by detection with the Tyramide Signal Amplification-Direct (Red) system (1:100, NEN Life Sciences). Sections were then incubated overnight with anti-Aβ (1:100), followed by incubation with FITC-conjugated avidin (1:75, Vector Laboratories).

The density of ChAT-positive neurons and of neurons with hSYN-immunoreactive inclusions was determined morphometrically. Two immunoperoxidase-stained sections were analyzed per mouse and antigen, and four light microscopic images (0.1 mm^2 each) were acquired per section. The threshold was set to detect only positively stained cells, and objects were counted automatically with the Quantimet 570C. The results from eight images per mouse were averaged and expressed as numbers per mm^2. The area occupied by 3D6-immunoreactive Aβ deposits was quantitated as described (17). Three immunolabeled sections were analyzed per mouse, and the average of the individual measurements was used to calculate group means.

Confocal microscopy was carried out as described (23) with a Zeiss 63× (numerical aperture 1.4) objective on an Axiovert 35 microscope (Zeiss) mounted on a MRC1024 laser scanning confocal microscope (Bio-Rad). The average percent area occupied by synaptophysin-immunoreactive presynaptic terminals of defined signal intensity (SIPT) was determined as described (17). Three sections were analyzed per mouse and four confocal images (7, 282 μm^2 each) of the neocortex and of the caudate/putamen per section.

Some Vibratome sections were postfixed with 2% glutaraldehyde/0.1% osmium tetroxide in 0.1 M sodium cacodylate buffer, embedded in epoxy, and analyzed with a Zeiss EM10 electron microscope as described (23). For immunogold cytochemistry (14), Vibratome sections were fixed in 0.25% glutaraldehyde and 3% paraformaldehyde in 0.1 M cacodylate buffer (pH 7.4). From each mouse, the temporal cortex was dissected and placed in gelatin capsules containing a polymerized layer of LR white (medium grade, Ted Pella, Redding, CA). Blocks were sectioned with an Ultracut E, and thin sections (60–90 Å) were placed on nickel grids coated with 0.5% Parlodion film. Grids were incubated with anti-Aβ (3D6) or anti-hSYN (72–10) followed by rabbit anti-mouse-gold or goat anti-rabbit-gold (5 nm, Zymed), respectively. Immunogold-labeled grids were examined with a Zeiss EM10 electron microscope. In control experiments, grids were incubated with gold-labeled secondary antibodies in the absence of primary antibody.

Statistics. Mice, sections, and samples were analyzed in a blind-coded fashion. Statistical analyses were performed with STATVIEW 5.0 (SAS Institute, Cary, NC). Null hypotheses were rejected at the 0.05 level.

Results and Discussion

Coexpression of hSYN and hAPP *in Vivo*. Heterozygous tg hSYN mice and hAPP mice (Fig. 1 *a* and *b*) with high levels of neuronal hSYN (line D) (23) or Aβ (line J9) (17) production, respectively, were crossed to obtain four groups of littermates: hSYN mice (n = 26), hAPP mice (n = 32), hSYN/hAPP mice (n = 21), and non-tg controls (n = 31). Levels of transgene-derived mRNAs in the brain were similar in singly and doubly tg mice (Fig. 1*c*), indicating that coexpression of hSYN and hAPP did not alter transgene expression. At the protein level, expression of hSYN did not affect hAPP expression in doubly tg mice (Fig. 1*d*). Cerebral hSYN levels tended to be higher in hSYN/hAPP mice than in hSYN mice (Fig. 1*d*). In addition, the levels of apparent hSYN oligomers and larger hSYN aggregates were higher in hSYN/hAPP mice than in hSYN mice (Fig. 1*d* and data not shown).

Neurological Deficits in hSYN/hAPP Mice. Motor deficits were assessed with the rotarod test as described (23). At 6 months of age,

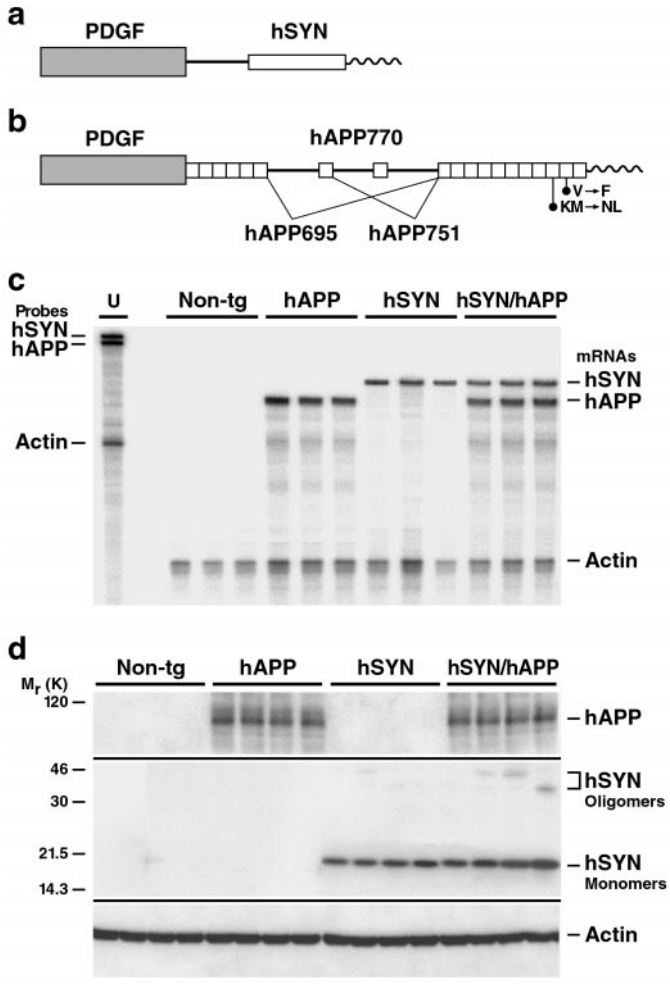

Fig. 1. Expression of hSYN and hAPP in brains of tg mice. (*a* and *b*) Neuronal expression of a hSYN cDNA (*a*) and an alternatively spliced hAPP minigene (*b*) was directed by the human platelet-derived growth factor β-chain promoter as described (17, 23, 25). Elements are not drawn to scale. hSYN/hAPP doubly tg mice were obtained from crosses between previously established lines: hSYN line D (23) and hAPP line J9 (17, 50). Line J9 carries familial Alzheimer's disease (FAD)-linked mutations ($670/671_{KM\rightarrow NL}$ and $717_{V\rightarrow F}$, hAPP770 numbering) that increase the production of Aβ1–40 and Aβ1–42. (*c*) Cerebral levels of transgene-derived mRNAs. Total RNA was extracted from hemibrains of 4-month-old mice and analyzed by RNase protection assay. The leftmost lane shows signals of undigested radiolabeled riboprobes (U). The lanes to the right contained the same riboprobes plus brain RNA (10 μg per lane) from different mice, digested with RNases. Protected mRNA segments are identified on the right. Signals were quantitated by phosphorimager analysis: singly and doubly tg mice ($n = 3$ per genotype) did not differ significantly in hSYN/actin (0.77 ± 0.11 vs. 0.82 ± 0.25) or hAPP/actin (1.60 ± 0.27 vs. 1.33 ± 0.21) ratios (mean $\pm$ SD). (*d*) Cerebral levels of hAPP, hSYN, and mouse actin. Frontal cortex homogenates of 4-month-old mice ($n = 4$ per genotype) were separated into cytosolic (for hSYN) and particulate (for hAPP) fractions (12 μg per lane), resolved by SDS/10% PAGE, and subjected to Western blot analysis as described (23). hSYN was detected with 72–10 (1:1000) and hAPP with 8E5 (1:2500). Blots were cropped as indicated by horizontal lines. Anti-actin (MAB1501, 1:500) labeling of stripped hSYN (not shown) and hAPP (bottom) blots confirmed equal loading of lanes. Longer exposures of the full-length hSYN blot revealed apparent hSYN oligomers, as well as higher molecular weight hSYN aggregates, in hSYN/hAPP mice and, at much lower levels, also in hSYN singly tg mice (data not shown).

hSYN/hAPP mice already showed significant deficits relative to non-tg controls ($P < 0.03$ by repeated measures ANOVA), whereas hSYN mice did not (Fig. 2*a*). At 12 months of age, both hSYN/hAPP and hSYN mice showed deficits in this test compared with non-tg controls ($P < 0.001$ by repeated-measures ANOVA) (Fig. 2*b*). hAPP mice had no significant motor deficits at either age. The severity of motor deficits was similar in 6-month-old hSYN/hAPP and 12-month-old hSYN and hSYN/hAPP mice, suggesting that hAPP/Aβ accelerates the development of hSYN-dependent motor deficits.

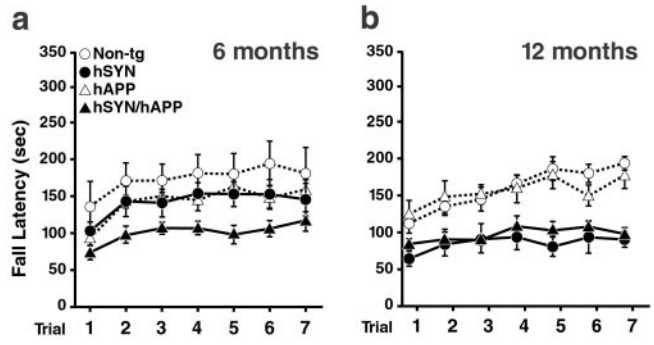

Fig. 2. hAPP/Aβ accelerates hSYN-dependent motor deficits. Male mice, 6 (*a*) or 12 (*b*) months of age ($n = 6$–8 per age and genotype), were assessed in the rotarod test as described (23). After an initial adaptation period, fall latencies were recorded in seven consecutive trials (10-min intertrial intervals). Compared with age-matched non-tg controls, only hSYN/hAPP mice were significantly impaired at 6 months whereas both hSYN and hSYN/hAPP mice were impaired at 12 months.

To determine the effects of hSYN and hAPP/Aβ on spatial learning and memory, we assessed the mice in a water maze test (Fig. 3). All groups of mice were able to locate a visible platform equally well (Fig. 3*a*), indicating that the motor deficits of hSYN/hAPP do not preclude normal performance in this test. In the hidden platform sessions, mice must use their memory of visual cues outside of the maze to find the submerged platform. In these sessions, hSYN/hAPP mice showed the most significant learning deficits, whereas hSYN mice and non-tg controls performed normally (Fig. 3*a*). The probe trial, during which the platform is removed, provides a putative measure of spatial memory retention. In this trial, hSYN/hAPP mice and hAPP

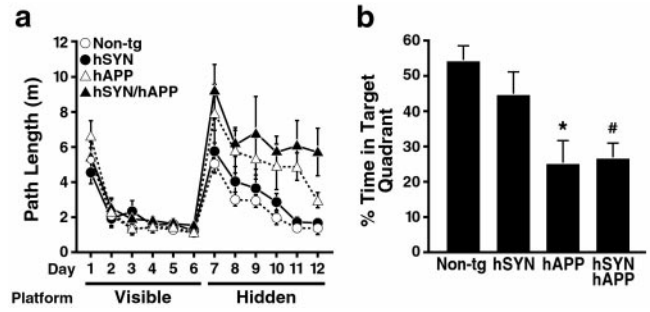

Fig. 3. hSYN/hAPP mice have severe learning deficits in the water maze test. (*a*) Six-month-old male mice ($n = 6$ per genotype) were first trained for 6 days to find a visible platform. All groups of mice acquired this task equally well, demonstrating that the motor deficits observed at this age in hSYN/hAPP mice (Fig. 2) did not interfere with their performance in the water maze test. On day 7 of training, the platform was hidden under the opaque water to test the ability of the mice to use visual cues outside of the maze to locate the hidden platform. Non-tg and hSYN mice learned to locate the hidden platform, whereas hAPP mice were impaired ($P = 0.023$ vs. non-tg by repeated-measures ANOVA). hSYN/hAPP mice had even more significant difficulties learning this task ($P = 0.0094$ vs. non-tg by repeated-measures ANOVA). (*b*) After removal of the platform for a probe trial on day 13, hAPP and hSYN/hAPP mice spent less time searching in the target quadrant than non-tg controls, consistent with impaired retention of spatial memory. *, $P < 0.05$ vs. non-tg mice (Tukey–Kramer test). #, $P < 0.05$ vs. non-tg mice (Student Neuman–Keuls test).

NEUROBIOLOGY

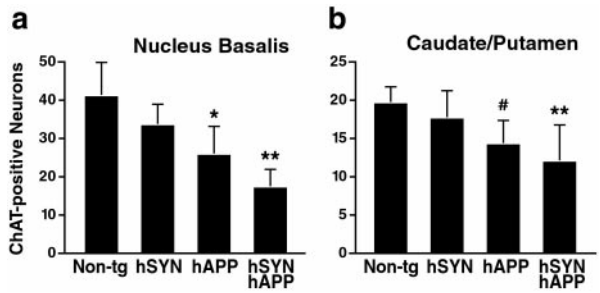

Fig. 4. Loss of cholinergic neurons in hAPP and hSYN/hAPP mice. Brain sections ($n = 2$ per mouse) of 20- to 22-month-old mice ($n = 3$–7 per genotype) were labeled with an antibody to ChAT, and the nucleus basalis (*a*) and caudate/putamen (*b*) were analyzed by light microscopy and morphometry. For each mouse, eight images were analyzed, and the results were used to calculate the average number of immunostained cells per mm^2 (mean ± SD). *, $P < 0.05$; **, $P < 0.01$ vs. non-tg controls (Tukey–Kramer test); #, $P < 0.05$ vs. non-tg controls (Student Neuman–Keuls test).

mice showed significantly less preference for the target quadrant than non-tg controls, suggesting impaired memory retention; hSYN mice were not impaired (Fig. 3*b*).

These results indicate that the motor deficits of hSYN/hAPP mice are caused primarily by hSYN, whereas their deficits in spatial learning and memory are caused primarily by hAPP/Aβ. Similar effects of hSYN and hAPP/Aβ may contribute to Lewy-body diseases, which also combine motor and cognitive deficits.

Age-Dependent Neurodegeneration. Degeneration of cholinergic neurons in the nucleus basalis of Meynert results in acquisition deficits in the water maze task in rodents (29). It is also a potentially important determinant of cognitive decline in AD and Lewy-body diseases (30, 31). ChAT mediates the synthesis of acetylcholine and serves as a marker of cholinergic neurons. We determined the density of ChAT-immunoreactive neurons in the nucleus basalis of our tg models (n = 13–17 mice/genotype, age range: 4–22 months). Simple regression analysis revealed a significant correlation between aging and loss of ChAT-positive neurons in hSYN mice ($r = 0.6$, $P < 0.03$), hAPP mice ($r = 0.66$, $P < 0.01$), and hSYN/hAPP mice ($r = 0.86$, $P < 0.0001$), but not in non-tg controls ($r = 0.22$, $P > 0.4$). The greatest loss was observed in aged hSYN/hAPP mice (Fig. 4*a*), which had fewer ChAT-positive neurons than aged hAPP mice ($P < 0.03$ by unpaired Student's t test). These results are consistent with the observation that cholinergic deficits are more severe in human patients with the Lewy-body variant of AD than in patients with pure AD (30). hSYN/hAPP mice and hAPP mice also had a significant loss of cholinergic neurons in the caudate/putamen (Fig. 4*b*), consistent with the decreased ChAT activity in the caudate of AD patients with or without Lewy bodies (30).

People with AD or the Lewy-body variant of AD typically also develop a significant loss of synapses in the neocortex, which is reflected in decreased synaptophysin immunoreactivity (31–33). We measured SIPT in the neocortex of 4- to 20-month-old mice (n = 15–19 per genotype). There was a significant negative correlation between aging and neocortical SIPT levels in hAPP mice ($r = 0.744$, $P = 0.0006$) and hSYN/hAPP mice ($r = 0.524$, $P = 0.021$), but not in hSYN mice ($r = 0.479$, $P = 0.071$) or non-tg controls ($r = 0.151$, $P = 0.564$). At 20 months of age, SIPT levels in the neocortex (percent area occupied, mean ± SD, n = 3–4 mice/genotype) were highest in non-tg controls (25.6 ± 0.9) and lowest in hSYN/hAPP mice (18.3 ± 4.8, $P < 0.05$ by Tukey–Kramer test), with values for hAPP mice (20.9 ± 1.7) and hSYN mice (23.0 ± 0.9) in between. In contrast, SIPT levels in the caudate/putamen at 20 months were normal in non-tg mice (27.1 ± 1.5) and hAPP mice (25.1 ± 3.6), but decreased in hSYN

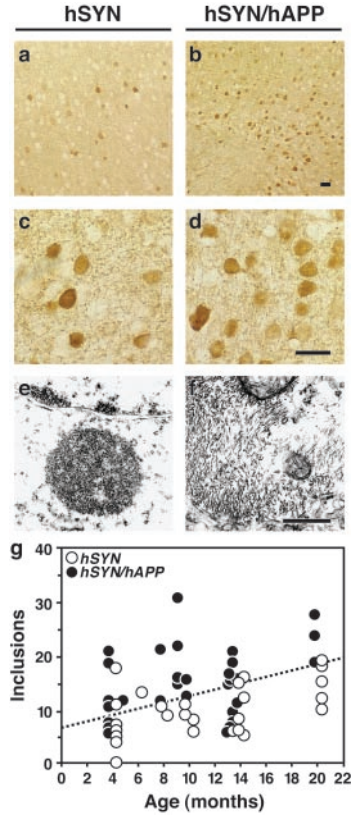

Fig. 5. Increased number and fibrillar characteristics of neuronal inclusions in hSYN/hAPP mice. (*a*–*d*) Brain sections were labeled with an antibody against hSYN (72–10) and analyzed by light microscopy. hSYN/hAPP mice (*b* and *d*) had more hSYN-immunoreactive neuronal inclusions in the temporal cortex (depicted here) and in the cingulate cortex (not shown) than hSYN mice (*a* and *c*). Images are from 12-month-old mice. (Scale bars, 20 μm.) (*e* and *f*) Sections of temporal cortex from 12-month-old hSYN (e) or hSYN/hAPP (*f*) mice were analyzed by transmission electron microscopy. Images depict intraneuronal inclusions. (Scale bar, 1 μm.) (*g*) hSYN-immunoreactive neuronal inclusions increased with age in both hSYN ($r = 0.51$, $P = 0.006$) and hSYN/hAPP ($r = 0.39$, $P = 0.027$) mice. Each dot represents measurements obtained in the temporal cortex of a different mouse expressed as average number of hSYN-immunoreactive inclusions per mm^2.

mice (21.0 ± 0.9) and hSYN/hAPP mice (20.1 ± 1.7) ($P < 0.05$ vs. non-tg controls by Tukey–Kramer test).

Thus, the age-dependent loss of cholinergic neurons in hSYN/hAPP mice depends primarily on hAPP/Aβ, with hSYN having some additive effects in the nucleus basalis. The age-dependent loss of SIPT in the neocortex of these mice is also due primarily to hAPP/Aβ with minor contributions from hSYN. Loss of SIPT in the basal ganglia is due almost entirely to hSYN.

Aβ Promotes Accumulation of hSYN. Accumulation of hSYN within neurons is a hallmark of Lewy-body diseases, including the Lewy-body variant of AD. An age-dependent accumulation of hSYN occurs in neurons of hSYN singly tg mice (23). Between 4 and 20 months of age, the number of neuronal inclusions in the neocortex was on average 1.6-fold higher in hSYN/hAPP mice than in age-matched hSYN mice (15.3 ± 1.1 vs. 9.5 ± 0.9 per mm^2, n = 28–32 mice per genotype, mean ± SEM, $P = 0.0002$ by unpaired two-tailed Student's t test). This is illustrated for 12-month-old mice in Fig. 5 *a*–*d*. The number of inclusions increased with age in both hSYN and hSYN/hAPP mice (Fig. 5*g*). These results indicate that hAPP/Aβ enhances the accumulation of hSYN in neurons.

By ultrastructural analysis, all intraneuronal inclusions in

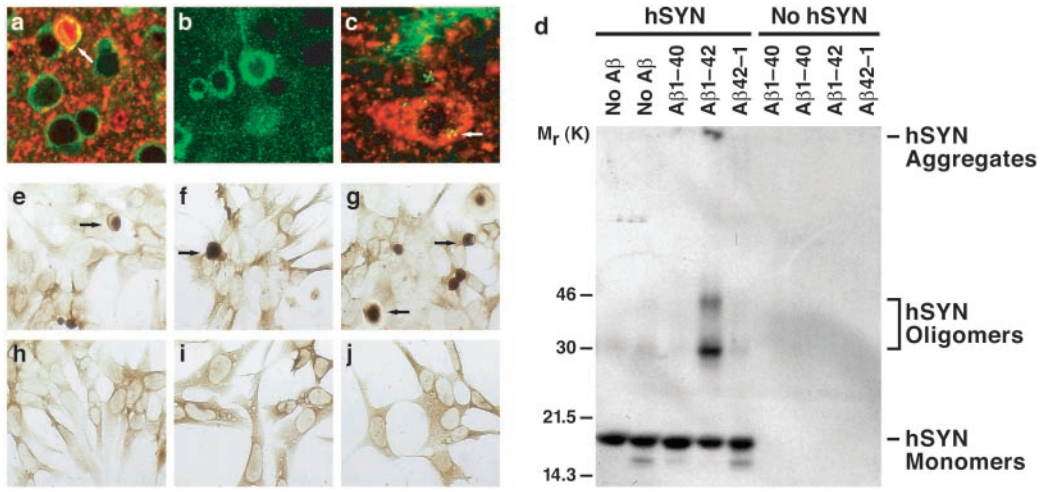

Fig. 6. Role of hAPP/Aβ in the accumulation of hSYN *in vivo* and *in vitro*. (*a–c*) Sections of temporal cortex from 12-month-old hSYN/hAPP (*a* and *c*) or hAPP (*b*) mice were double-labeled with antibodies against hSYN (red) and hAPP (green) (*a* and *b*) or against hSYN (red) and Aβ (green) (*c*) and analyzed by confocal microscopy. Note the colabeling for hAPP and hSYN (yellow) of the neuron (arrow) containing a dense hSYN accumulation (*a*) and the close association of Aβ deposits (green granules) with intracellular hSYN accumulations (red) (*c*). All images were obtained at a magnification of ×930. The image in *c* was magnified electronically to better visualize Aβ-immunoreactive granules. (*d*) Recombinant hSYN (10 μM final concentration) was or was not mixed with freshly solubilized synthetic Aβ1–40, Aβ1–42, or control peptide of reverse sequence (Aβ42–1) (each at a final concentration of 10 μM) in 20 μl of 100 mM Tris·HCl buffer (pH 7.5). All samples were incubated at 37°C for 24 h and then subjected to SDS/15% PAGE. After blotting of samples onto nitrocellulose membrane, the membrane was blocked with Tris-buffered saline (TBS; 20 mM Tris·HCl, pH 7.5/150 mM NaCl) containing 3% BSA, followed by incubation with anti-hSYN (1:1000) in TBS containing 1% BSA. The membrane was then incubated with ^{125}I-labeled protein A (ICN), followed by autoradiography. (*e–j*) Neuronal GT1–7 cells stably transfected with SYN cDNA (*e–g*) or control plasmid (*h–j*) as described (27), were left untreated (*e* and *h*) or exposed for 48 h to Aβ1–40 (*f* and *i*), Aβ1–42 (*g* and *j*), or Aβ42–1 (not shown) at 2 μM final concentration, followed by immunoperoxidase staining with anti-SYN (27).

hSYN mice were amorphous and electrodense (Fig. 5*e*, and ref. 23), whereas ≈15% of the intraneuronal inclusions in hSYN/hAPP were fibrillar (Fig. 5*f*), increasing their resemblance to Lewy bodies in the human condition (34, 35). Filamentous inclusions in the neuronal cytoplasm were labeled when brain sections of hSYN/hAPP mice were analyzed by immunogold electron microscopy with anti-hSYN or anti-Aβ (data not shown). These results suggest that Aβ may promote the *in vivo* fibrillization of hSYN by direct interaction. Further supporting this possibility, Aβ-immunoreactive granular deposits were detected by confocal microscopy in hSYN-positive intraneuronal inclusions in hSYN/hAPP mice (Fig. 6*c*).

To further evaluate whether the alterations observed in hSYN/hAPP mice could indeed result from direct interactions between Aβ and hSYN, we extended our *in vivo* analysis to two *in vitro* models. In a cell-free system, Aβ1–42 strongly promoted the formation of presumed hSYN oligomers and high molecular weight hSYN polymers (Fig. 6*d*), consistent with previous observations (36). This effect was observed with both aged (putatively aggregated) and freshly solubilized Aβ1–42. However, because Aβ1–42 aggregates rapidly in aqueous solutions, we cannot be certain that the effect was independent of the aggregation state of Aβ1–42. Interestingly, the less fibrillogenic Aβ1–40 did not affect hSYN aggregation *in vitro* (Fig. 6*d*).

Aβ1–42 and Aβ1–40 also had different effects on the intracellular accumulation of SYN in neuronal cell cultures when added to the culture medium (Fig. 6 *e–j*). The percentage of cells with SYN-immunoreactive inclusions was higher in cultures treated with Aβ1–42 (55.4 ± 10.3) than in untreated cultures (21.4 ± 6.4) or cultures treated with Aβ1–40 (19.9 ± 4.8) or Aβ42–1 (19.4 ± 5.2) (mean ± SD, $P < 0.05$ by Tukey–Kramer test).

Overproduction of Aβ1–42 within the endoplasmic reticulum and intermediate compartment (10) may interfere with the processing of SYN, enhancing its accumulation. However, our cell culture data demonstrate that extracellular exposure to Aβ1–42 is sufficient to induce the intracellular accumulation of SYN, whereas exposure to Aβ1–40 is not. Interestingly, cellular uptake of extracellular Aβ1–42, but not Aβ1–40, disrupted the integrity of lysosomal membranes (37, 38). Moreover, the association of soluble SYN with planar lipid bilayers results in extensive bilayer disruption (39). The combined action of Aβ1–42 and SYN could cause endosomal–lysosomal membranes to leak, allowing for direct interactions between Aβ1–42 and SYN in the cytosol. As demonstrated by our *in vitro* findings, such an interaction could promote the intracellular accumulation of SYN. This effect of Aβ1–42 on SYN might be mediated by direct fibrillogenic interactions between these molecules (40) or by free radicals. Aβ may exert oxidative stress (41), and growing evidence suggests that oxidative crosslinking of SYN contributes to Lewy-body formation (9, 42). These possibilities are not mutually exclusive and deserve to be tested further in future studies.

In contrast to the prominent effects of Aβ on SYN accumulation, hSYN expression did not significantly alter the extracellular deposition of Aβ into plaques or the development of plaque-associated neuritic dystrophy in 8-, 12-, or 20-month-old hSYN/hAPP mice compared with age-matched hAPP mice (n = 3–4 mice per genotype and age). Twelve-month-old hAPP mice and hSYN/hAPP mice had similar cerebral levels of Aβ1–40 (4.3 ± 0.88 vs 4.6 ± 0.6) and Aβ1–42 (248 ± 48 vs 275 ± 41) as determined by ELISA (μg/g of hemibrain, mean ± SD, n = 4–11 mice per genotype).

Conclusions

hSYN/hAPP mice have cognitive and motor alterations, loss of cholinergic neurons and SIPT, extensive amyloid plaques, and hSYN-immunoreactive intraneuronal fibrillar inclusions. All of these features are also found in the Lewy-body variant of AD (2, 30, 43, 44). Interestingly, ≈25% of patients with AD develop frank parkinsonism (3), and hSYN-immunoreactive Lewy-body-like inclusions develop in most cases of sporadic AD and FAD, as well as in Down's syndrome, which is associated with early onset AD (45, 46). Moreover, Lewy bodies contain hAPP

(47–49). Our study demonstrates that hSYN and hAPP/Aβ have distinct, as well as convergent, pathogenic effects on the integrity and function of the brain. Although hSYN did not affect the Aβ-dependent development of neuritic plaques or the overall Aβ content in the brain, it worsened hAPP/Aβ-dependent cognitive deficits and neurodegeneration in specific brain regions. These findings indicate that hSYN may enhance the plaque-independent neurotoxicity of Aβ (17, 50, 51). They help explain the clinical observation that the Lewy-body variant of AD causes a more rapid cognitive decline than pure AD (30).

Overexpression of hAPP/Aβ, in turn, promoted the intraneuronal accumulation of hSYN and accelerated the development of motor deficits in tg mice. Although we cannot be certain whether these effects were mediated by Aβ or another hAPP product, our *in vitro* studies strongly suggest that Aβ1–42 is the predominant culprit. It remains to be determined whether the neuronal deficits in these models and the corresponding human diseases are dependent on fibrillar or prefibrillar forms of Aβ and hSYN (17, 50–52). In either case, the pathogenic interactions between Aβ and hSYN demonstrated here suggest that drugs aimed at blocking the accumulation of Aβ or hSYN might benefit a broader spectrum of neurodegenerative disorders than previously anticipated.

Note Added in Proof. Since the acceptance of our paper, two reports have appeared demonstrating that Aβ1-42 promotes the aggregation of tau into neurofibrillary tangles (53, 54). These results are consistent with the effects of Aβ1-42 on α-synuclein aggregation we identified in the current study. Taken together, these findings suggest that Aβ1-42 might contribute to diverse conformational diseases.

We thank Pamela Mellon for the GT1–7 cell line, Peter Seubert and Dora Games for antibodies against APP and Aβ, Steve Finkbeiner and Fen-Biao Gao for helpful comments on the manuscript, John Carroll for preparation of graphics, Stephen Ordway and Gary Howard for editorial assistance, and Denise McPherson for administrative assistance. This work was supported by National Institutes of Health Grants AG11385, AG5131, AG10869, and AG18440, and Zenith Award from the Alzheimer's Association (to L.M.).

1. Ditter, S. M. & Mirra, S. S. (1987) *Neurology* **37,** 754–760.
2. Hansen, L., Salmon, D., Galasko, D., Masliah, E., Katzman, R., DeTeresa, R., Thal, L., Pay, M. M., Hofstetter, R. & Klauber, M. (1990) *Neurology* **40,** 1–8.
3. Galasko, D., Hansen, L. A., Katzman, R., Wiederholt, W., Masliah, E., Terry, R., Hill, L. R., Lessin, P. & Thal, L. J. (1994) *Arch. Neurol.* **51,** 888–895.
4. Terry, R. D., Katzman, R., Bick, K. L. & Sisodia, S. S. (1999) *Alzheimer Disease* (Lippincott, Philadelphia).
5. Lang, A. E. & Lozano, A. M. (1998) *N. Engl. J. Med.* **339,** 1044–1143.
6. Seabrook, G. R., Smith, D. W., Bowery, B. J., Easter, A., Reynolds, T., Fitzjohn, S. M., Morton, R. A., Zheng, H., Dawson, G. R., Sirinathsinghji, D. J. S., *et al.* (1999) *Neuropharmacology* **38,** 349–359.
7. Clayton, D. F. & George, J. M. (1998) *Trends Neurosci.* **21,** 249–254.
8. Goedert, M., Spillantini, M. G. & Davies, S. W. (1998) *Curr. Opin. Neurobiol.* **8,** 619–632.
9. Giasson, B. I., Duda, J. E., Murray, I. V. J., Chen, Q. P., Souza, J. M., Hurtig, H. I., Ischiropoulos, H., Trojanowski, J. Q. & Lee, V. M. Y. (2000) *Science* **290,** 985–989.
10. Wilson, C. A., Doms, R. W. & Lee, V. M.-Y. (1999) *J. Neuropathol. Exp. Neurol.* **58,** 787–794.
11. Selkoe, D. J. (2001) *Physiol. Rev.* **81,** 741–766.
12. Huber, G., Bailly, Y., Martin, J. R., Mariani, J. & Brugg, B. (1997) *Neuroscience* **80,** 131–320.
13. Games, D., Adams, D., Alessandrini, R., Barbour, R., Berthelette, P., Blackwell, C., Carr, T., Clemens, J., Donaldson, T., Gillespie, F., *et al.* (1995) *Nature (London)* **373,** 523–527.
14. Masliah, E., Sisk, A., Mallory, M., Mucke, L., Schenk, D. & Games, D. (1996) *J. Neurosci.* **16,** 5795–5811.
15. Price, D. L. & Sisodia, S. S. (1998) *Annu. Rev. Neurosci.* **21,** 479–505.
16. Dodart, J. C., Meziane, H., Mathis, C., Bales, K. R., Paul, S. M. & Ungerer, A. (1999) *Behav. Neurosci.* **113,** 982–990.
17. Mucke, L., Masliah, E., Yu, G.-Q., Mallory, M., Rockenstein, E. M., Tatsuno, G., Hu, K., Kholodenko, D., Johnson-Wood, K. & McConlogue, L. (2000) *J. Neurosci.* **20,** 4050–4058.
18. Polymeropoulos, M. H., Lavedan, C., Leroy, E., Ide, S. E., Dehejia, A., Dutra, A., Pike, B., Root, H., Rubenstein, J., Boyer, R., *et al.* (1997) *Science* **276,** 2045–2047.
19. Krüger, R., Kuhn, W., Müller, T., Woitalla, D., Graeber, M., Kösel, S., Przuntek, H., Epplen, J. T., Schöls, L. & Riess, O. (1998) *Nat. Genet.* **18,** 106–108.
20. Spillantini, M. G., Schmidt, M. L., Lee, V. M.-Y., Trojanowski, J. Q., Jakes, R. & Goedert, M. (1997) *Nature (London)* **388,** 839–840.
21. Wakabayashi, K., Matsumoto, K., Takayama, K., Yoshimoto, M. & Takahashi, H. (1997) *Neurosci. Lett.* **239,** 45–48.
22. Takeda, A., Mallory, M., Sundsmo, M., Honer, W., Hansen, L. & Masliah, E. (1998) *Am. J. Pathol.* **152,** 367–372.
23. Masliah, E., Rockenstein, E., Veinbergs, I., Mallory, M., Hashimoto, M., Takeda, A., Sagara, Y., Sisk, A. & Mucke, L. (2000) *Science* **287,** 1265–1269.
24. Feany, M. B. & Bender, W. W. (2000) *Nature (London)* **404,** 394–398.
25. Rockenstein, E. M., McConlogue, L., Tan, H., Gordon, M., Power, M., Masliah, E. & Mucke, L. (1995) *J. Biol. Chem.* **270,** 28257–28267.
26. Mellon, P. L., Windle, J. J., Goldsmith, P. C., Padula, C. A., Roberts, J. L. & Weiner, R. I. (1990) *Neuron* **5,** 1–10.
27. Hsu, L. J., Sagara, Y., Arroyo, A., Rockenstein, E., Sisk, A., Mallory, M., Wong, J., Takenouchi, T., Hashimoto, M. & Masliah, E. (2000) *Am. J. Pathol.* **157,** 401–410.
28. Johnson-Wood, K., Lee, M., Motter, R., Hu, K., Gordon, G., Barbour, R., Khan, K., Gordon, M., Tan, H., Games, D., *et al.* (1997) *Proc. Natl. Acad. Sci. USA* **94,** 1550–1555.
29. Mandel, R. J., Gage, F. H. & Thal, L. J. (1989) *Exp. Neurol.* **104,** 208–217.
30. Langlais, P. J., Thal, L., Hansen, L., Galasko, D., Alford, M. & Masliah, E. (1993) *Neurology* **43,** 1927–1934.
31. Samuel, W., Alford, M., Hofstetter, C. R. & Hansen, L. (1997) *J. Neuropathol. Exp. Neurol.* **56,** 499–508.
32. Terry, R. D., Masliah, E., Salmon, D. P., Butters, N., DeTeresa, R., Hill, R., Hansen, L. A. & Katzman, R. (1991) *Ann. Neurol.* **30,** 572–580.
33. Brown, D. F., Risser, R. C., Bigio, E. H., Tripp, P., Stiegler, A., Welch, E., Eagan, K. P., Hladik, C. L. & White, C. L. I. (1998) *J. Neuropathol. Exp. Neurol.* **57,** 955–960.
34. Kuzuhara, S., Mori, H., Izumiyama, N., Yoshimura, M. & Ihara, Y. (1988) *Acta Neuropathol.* **75,** 345–353.
35. Serpell, L. C., Berriman, J., Jakes, R., Goedert, M. & Crowther, R. A. (2000) *Proc. Natl. Acad. Sci. USA* **97,** 4897–4902.
36. Paik, S. R., Lee, J.-H., Kim, D.-H., Chang, C.-S. & Kim, Y.-S. (1998) *FEBS Lett.* **421,** 73–76.
37. Yang, A. J., Chandswangbhuvana, D., Margol, L. & Glabe, C. G. (1998) *J. Neurosci. Res.* **52,** 691–698.
38. Yang, A. J., Chandswangbhuvana, D., Shu, T., Henschen, A. & Glabe, C. G. (1999) *J. Biol. Chem.* **274,** 20650–20656.
39. Jo, E. J., McLaurin, J., Yip, C. M., St. George-Hyslop, P. & Fraser, P. E. (2000) *J. Biol. Chem.* **275,** 34328–34334.
40. El-Agnaf, O. M. A. & Irvine, G. B. (2000) *J. Struct. Biol.* **130,** 300–309.
41. Varadarajan, S., Yatin, S., Aksenova, M. & Butterfield, D. A. (2000) *J. Struct. Biol.* **130,** 184–208.
42. Hashimoto, M., Hsu, L. J., Xia, Y., Takeda, A., Sisk, A., Sundsmo, M. & Masliah, E. (1999) *NeuroReport* **10,** 717–721.
43. McKeith, I. G., Galasko, D., Kosaka, K., Perry, E. K., Dickson, D. W., Hansen, L. A., Salmon, D. P., Lowe, J., Mirra, S. S., Byrne, E. J., *et al.* (1996) *Neurology* **47,** 1113–1124.
44. Bancher, C., Braak, H., Fischer, P. & Jellinger, K. A. (1993) *Neurosci. Lett.* **162,** 179–182.
45. Lippa, C. F., Schmidt, M. L., Lee, V. M. Y. & Trojanowski, J. Q. (1999) *Ann. Neurol.* **45,** 353–357.
46. Hamilton, R. L. (2000) *Brain Pathol.* **10,** 378–384.
47. Arai, H., Lee, V. M.-Y., Messinger, M. L., Greenberg, B. D., Lowery, D. E. & Trojanowski, J. Q. (1991) *Ann. Neurol.* **30,** 686–693.
48. Van Gool, D., De Strooper, B., Van Leuven, F. & Dom, R. (1995) *Dementia* **6,** 63–68.
49. Halliday, G., Brooks, W., Arthur, H., Creasey, H. & Broe, G. A. (1997) *Neurosci. Lett.* **227,** 49–52.
50. Hsia, A., Masliah, E., McConlogue, L., Yu, G., Tatsuno, G., Hu, K., Kholodenko, D., Malenka, R. C., Nicoll, R. A. & Mucke, L. (1999) *Proc. Natl. Acad. Sci. USA* **96,** 3228–3233.
51. Klein, W. L., Krafft, G. A. & Finch, C. E. (2001) *Trends Neurosci.* **24,** 219–224.
52. Rochet, J. C., Conway, K. A. & Lansbury, P. T., Jr. (2000) *Biochemistry* **39,** 10619–10626.
53. Lewis, J., Dickson, D. W., Lin, W. L., Chisholm, L., Corral, A., Jones, G., Yen, S. H., Sahara, N., Skipper, L., Yager, D., *et al.* (2001) *Science* **293,** 1487–1491.
54. Gotz, J., Chen, F., van Dorpe, J. & Nitsch, R. M. (2001) *Science* **293,** 1491–1494.